# Chaotic mixing of granular materials in two-dimensional tumbling mixers

D. V. Khakhar,[a] J. J. McCarthy,[b] J. F. Gilchrist, and J. M. Ottino[c]
*Department of Chemical Engineering, Northwestern University, Evanston, Illinois 60208*

(Received 15 July 1998; accepted for publication 30 December 1998)

We consider the mixing of similar, cohesionless granular materials in quasi-two-dimensional rotating containers by means of theory and experiment. A mathematical model is presented for the flow in containers of arbitrary shape but which are symmetric with respect to rotation by 180° and half-filled with solids. The flow comprises a thin cascading layer at the flat free surface, and a fixed bed which rotates as a solid body. The layer thickness and length change slowly with mixer rotation, but the layer geometry remains similar at all orientations. Flow visualization experiments using glass beads in an elliptical mixer show good agreement with model predictions. Studies of mixing are presented for circular, elliptical, and square containers. The flow in circular containers is steady, and computations involving advection alone (no particle diffusion generated by interparticle collisions) show poor mixing. In contrast, the flow in elliptical and square mixers is time periodic and results in chaotic advection and rapid mixing. Computational evidence for chaos in noncircular mixers is presented in terms of Poincaré sections and blob deformation. Poincaré sections show regions of regular and chaotic motion, and blobs deform into homoclinic tendrils with an exponential growth of the perimeter length with time. In contrast, in circular mixers, the motion is regular everywhere and the perimeter length increases linearly with time. Including particle diffusion obliterates the typical chaotic structures formed on mixing; predictions of the mixing model including diffusion are in good qualitative and quantitative (in terms of the intensity of segregation variation with time) agreement with experimental results for mixing of an initially circular blob in elliptical and square mixers. Scaling analysis and computations show that mixing in noncircular mixers is faster than that in circular mixers, and the difference in mixing times increases with mixer size.  [S1054-1500(99)02301-0]

**The fundamentals of granular mixing are not well understood, particularly in comparison with fluid mixing. We consider the mixing in two-dimensional tumbling mixers with a view to reveal the role of advection in the dynamics of mixing. Computations and experiments for noncircular mixers show chaotic advection, which results in faster convective mixing as compared to circular mixers. Chaotic advection dominates in large mixers, the norm for industrial processes, whereas particle diffusion is important for small—laboratory scale—mixers. The results are important for the design and scale-up of industrial mixers.**

## I. INTRODUCTION

Mixing of granular materials is an important operation in several industrial processes in the pharmaceutical, food, chemical, ceramic, metallurgical, and construction industries.[1] Examples range from blending active pharmaceutical compounds in filler material in the manufacture of tablets to heat transfer and reaction in rotary kilns in the manufacture of cement. Mixing of grains is also important in some natural processes such as the formation of sedimentary structures in marine basins.[2]

Granular mixing has been the subject of a number of studies beginning with the early work of Lacey.[3] A significant fraction of the works have been devoted to tumbling mixers—rotating containers partially filled with solids, which find wide application in industry for the blending of freely flowing granular materials. The approach in most such studies is to characterize the efficacy of mixers by determining the time evolution of a global mixing index, a statistical measure, which reflects the extent of mixing.[4] The index (several have been proposed—Ref. 5) is typically determined by sampling the composition at different (usually random) positions within the mixer. Significant advances have been made in sampling procedures and analysis of data.[6] This approach, however, gives little insight into the dynamics of mixing.

The fundamentals of the mixing of granular materials are poorly understood, particularly when compared to the mixing of fluids (see, e.g., Ref. 7). Consider first the case of similar cohesionless particles. Only a few studies on a prototypical system (a partially filled horizontal rotating cylinder) have focused on elucidating mechanisms—diffusion (arising from the random motions generated by interparticle collisions) and advection.[8–13] The behavior is different depending on the operating regime (which may be quantified in terms of the Froude number, $\mathrm{Fr}=\omega L^2/g$, where $g$ is the ac-

[a]Permanent address: Department of Chemical Engineering, Indian Institute of Technology Bombay, Powai, Mumbai 400076, India.
[b]Current address: Department of Chemical Engineering, University of Pittsburgh, Pittsburgh, PA 15260.
[c]Author to whom all correspondence should be addressed.

 

celeration due to gravity, $L$ is the length scale of the system, and $\omega$ the rotational speed. At low speeds (i.e., low Fr) corresponding to the avalanching regime, the flow is intermittent and comprises discrete time-periodic avalanches.[14] The transverse mixing in this case is dominated by geometry:[7] Each avalanche results in a wedge-shaped bed of particles at the free surface, abruptly cascading to form a new wedge at a lower position. To a first-order approximation the avalanche produces uniform mixing with a wedge, however, mixing at the scale of the cylinder results from wedge intersections. Thus, a half-full cylinder results in no wedge intersections and mixing is slow.[7]

At higher mixer rotational speeds, the continuous flow rolling regime[14] is obtained, in which a thin layer of particles flows down the free surface while the remaining particles rotate as a fixed bed. Particles continuously enter the layer from the fixed bed in the upper-half of the layer, and exit from the layer into the fixed bed in the lower half; the free surface in this regime remains flat. Transverse mixing in this case depends on dynamics and results from shearing and collisional diffusion within the layer.[9,10] Consider a blob of tracer particles which enters the layer. While passing through the layer the blob is sheared and becomes blurred due to collisional diffusion, it then enters the bed, and after a solid body rotation, it reenters the layer; and the process repeats. Mixing also has a geometric component: Particles at different radial positions may have different residence times in the bed and thus enter the layer at different times resulting in mixing. The differences in rotation times are the smallest for half-full mixers: In this case all the particles spend nearly the same time in the bed. Axial mixing occurs due to diffusion alone, since there is no axial flow.[11–13]

Differences in particle properties (e.g., size, density, shape, surface roughness, etc.) can result in spontaneous separation of the different particles during mixing.[14,15] Such granular segregation can occur by various mechanisms, and different segregated patterns (e.g., radial cores, axial bands, etc., in rotating cylinders) may be formed depending on the geometry of the flow.[16–21] The local rate of segregation in a mixture depends on the shearing and granular packing in the region, in addition to the differences in particle properties. Consequently, the flow plays a critical role in determining the final segregated state. Shear-induced phase separation in polymer blends is perhaps the closest analog of the segregation process in fluid mixing, although the physical processes are quite different. While the mechanisms of segregation are well understood in qualitative terms, only a few theoretical models are available to describe the process.[22–25]

The objective of the present work is to study the role of advection in granular mixing; we thus focus on mixtures of similar particles so that segregation does not occur. The implications of *simultaneous* mixing and segregation are discussed at the end of the paper.

The flow of similar particles in a rotating cylinder operating in the rolling regime is two dimensional (2D) and steady. Fluid mixing theory states that mixing in the system due to advection alone (no diffusion) is poor, since the streamlines are time invariant and closed, and act as impenetrable barriers.[26] Several studies on fluid mixing have shown that time modulation of a two-dimensional flow, such that superimposed streamlines at different times intersect, is sufficient to produce chaotic advection, which results in rapid mixing.[26] From a continuum viewpoint, the stretching of material elements is exponential with time in chaotic flows as compared to linear in steady 2D flows.

Producing chaotic advection in granular systems is relatively difficult. In contrast to fluid flows, granular flows are kinematically defined over most of the flow domain. Shearing of particles is confined to thin layers, while the rest of the particles move as a fixed bed with no relative motion between particles. This constrains, to a significant extent, the variations in flow that can be employed to improve mixing; analysis, however, is considerably simplified. One simple method of generating a time varying flow in a 2D tumbling mixer is to use mixers with noncircular cross sections. In this case the length and thickness of the cascading layer change with time resulting in the streamline modulation required for chaotic advection.

We analyze in this paper the flow and mixing of noncohesive granular materials in 2D tumbling mixers operating in the continuous flow rolling regime. The goal is to understand the role of mixer geometry in producing widespread chaotic advection, and the implications of chaotic mixing for practice. The role of advection is highlighted by means of model computations in which particle collisional diffusion is omitted (this is standard practice in the analysis of chaotic advection in fluids[7]). The effects of collisional diffusion, however, may be significant in many cases, and thus systems with simultaneous chaotic advection and collisional diffusion are considered as well. The paper is structured as follows. Transverse flow in 2D tumbling mixers is discussed in Sec. II, and the analysis of mixing in the system is given in Sec. III. The scale-up of tumbling mixers based on the model developed is discussed in Sec. IV, and the conclusions of the work are given in Sec. V.

## II. TRANSVERSE FLOW IN 2D TUMBLING MIXERS

### A. General problem

Consider the flow in a 2D tumbler of arbitrary, but everywhere convex (any two points in the mixer can be joined by a straight line without crossing the mixer boundary), cross-sectional shape as shown in Fig. 1. Rotation of the mixer about point $O$, at an angular speed $\omega$ in the rolling regime range, produces a thin layer of particles flowing down the free surface, which is nearly flat. The remaining particles rotate as a fixed bed. The angle of the free surface ($\beta$) remains constant in this regime (Fig. 1). Assume that the motion of the material interface normal to itself is small with respect to a coordinate system fixed at $O$. Continuity of the velocity field at the bed layer interface then allows the calculation of the velocities of the particles entering and leaving the layer, since the velocity in the bed is purely rotational and given by

$$v_r = 0, \quad v_\theta = \omega r \tag{1}$$

in cylindrical coordinates, with the origin at point $O$. The geometrical construction shown in Fig. 1 shows that the

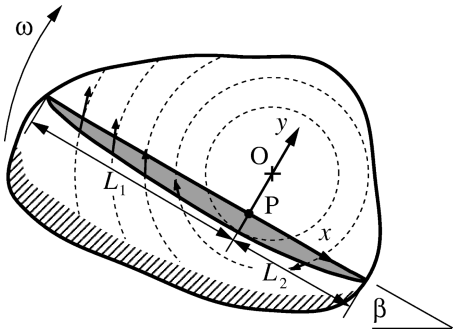


FIG. 1. Schematic view of continuous flow in a rotating mixer of arbitrary convex shape. The flowing layer is the shaded region, and the dashed lines show arcs of circles centered at point *O*. Velocity vectors for particles entering and leaving the bed are also shown. The mixer is rotated with angular velocity, $\omega$, about point *O* and the velocity profile within the layer is nearly simple shear.

point *P* on the surface closest to the axis of rotation demarcates the layer into two parts: Uphill of this point particles enter the layer from the bed whereas particles leave the layer and reenter the bed at downhill positions. For thin layers the velocity of the particles entering or leaving the layer is the component of the bed velocity normal to the bed–layer interface, and is given by

$$v_y = -\omega x \tag{2}$$

(Fig. 1). The particles then cascade down the layer, and the local downflow velocity determines the rate of change of the layer thickness.

The above analysis shows that the mass of the particles entering the layer at any time is, in general, different from that leaving the layer, and thus the local layer thickness and cascading velocity should vary in a complicated way. The geometry generates as well a variation of the layer length with time. Prediction of the time-varying flow in the system would require the (numerical) solution of the mass and momentum balance equations for the flow in the layer,[10] with the possible additional complication of momentum being generated by the up and down motion of the layer. The problem simplifies considerably for the case of half-filled convex containers, which are symmetric with respect to 180° rotations about their centroid, and an approximate analytical result is obtained. We confine most of the following discussion to this class.

### B. Specific case: Convex, rotationally symmetric, half-filled mixers

Two simplifications are apparent. First, since the mixer is half full, the point *P*, which demarcates the inflow and outflow regions, coincides with the centroid of the mixer *O* for all mixer orientations; and there is no up and down motion of the layer. Second, the layer is symmetric about the point *P*. Specifically $L_1 = L_2$ (Fig. 1) and the total flux of particles entering the layer from the uphill surface is exactly equal to that leaving from the downhill surface at any time. This is illustrated for a half-filled symmetric mixer of arbitrary shape shown in Fig. 2. If we now assume that the layer geometry changes slowly with time compared to the dynamics of the flow, the flow in the layer is quasisteady and similar to that for a circular mixer with the same layer geometry. Several previous experimental[27–29] and computational[30–32] studies have considered the flow in a rotating cylinder. A continuum model for the flow has recently been proposed,[10] which is consistent with previous experimental results, and the predictions of the model are in good agreement with experimental data. We review this model below.

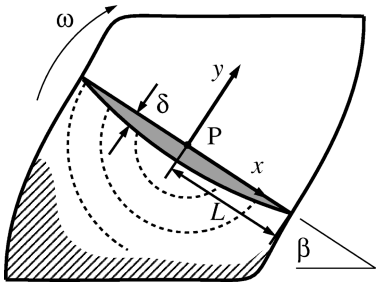


FIG. 2. Schematic view of flow in a rotating mixer of arbitrary convex shape which is symmetric with respect to half rotations and is half-filled. The layer in this case is symmetric about the point *P*, and material entering the layer ($x<0$) is equal to the material leaving the layer ($x>0$).

The velocity field in the layer obtained from the continuum model for a circular cylinder is

$$v_x = 2u\left(1+\frac{y}{\delta}\right), \tag{3}$$

$$v_y = -\omega x\left(\frac{y}{\delta}\right)^2, \tag{4}$$

where $u$ is the mean downflow velocity in the layer which, in general, varies with distance along the layer ($x$). Computations and experimental results indicate that the layer thickness may be approximated as $\delta = \delta_0[1-(x/L)^2]$, where $\delta_0$ is the midlayer thickness.[10] Using this expression for the layer thickness profile, together with the volume flux in the layer $Q = Q_0[1-(x/L)^2]$, obtained from the integration of the linear variation of the flux into the layer [Eq. (4)], gives $u = Q/\delta \equiv$ constant (a slightly more detailed model is given in Ref. 33).

There is an easier way to arrive at some of the above results. When the bed is half full, the entire bed passes through the layer in half a revolution of the mixer, so that the volumetric flow rate per unit cylinder length calculated at the midpoint of the layer ($x=0$) is

$$Q_0 = \frac{\pi L^2}{2}\frac{1}{(\pi/\omega)} = \frac{\omega L^2}{2}. \tag{5}$$

The average velocity is thus

$$u = \frac{\omega L^2}{2\delta_0} \tag{6}$$

and is inversely related to the midlayer thickness ($\delta_0$). If we assume that the $v_x$ flow is linear in $y$ we arrive at (3), and if a shape for $\delta$, $\delta = \delta(x)$, is assumed, by continuity we obtain $v_y$. The result given by (4) corresponds to a parabolic $\delta(x)$.

The governing equations for the flow in noncircular mixers in the quasisteady state are identical to the above, but

with the layer length ($L$), the midlayer thickness ($\delta_0$), and the mean velocity ($u$), all varying slowly with time. The variation of the layer length with time is uniquely determined by the mixer geometry. Assuming geometrical similarity of the layer at different times, we have $\delta_0(t)/L(t)=k \equiv$ constant (as we shall see experiments indicate that this is indeed true). This gives the variation of the mean velocity with time as

$$u(t)=\frac{\omega L(t)}{2k}. \tag{7}$$

Rotation of the mixer results in a periodic increase and decrease of the layer size, maintaining geometrical similarity; the mean velocity increases and decreases proportionately to the layer length. The flow becomes time invariant if all distances are scaled with $L(t)$, and velocities with $\omega L(t)$.

Consider next the variation of layer length for specific mixer geometries. For an ellipse we obtain

$$L(t)=\frac{ab}{[b^2\cos^2(\omega t+\alpha)+a^2\sin^2(\omega t+\alpha)]^{1/2}}, \tag{8}$$

where $a$ and $b$ are the major and minor semiaxes of the ellipse, respectively, and $\alpha$ is the initial angle between the free surface and the major axis of the ellipse. Similarly, for a rectangular mixer we have

$$L(t)=\begin{cases}\dfrac{a}{|\cos\theta|} & \text{if } \theta<\theta_d \text{ or } |\pi-\theta|<\theta_d \text{ or } \theta>(2\pi-\theta_d)\\ \dfrac{b}{|\sin\theta|} & \text{otherwise}\end{cases} \tag{9}$$

where $\theta=(\omega t+\alpha)\mathrm{mod}(2\pi)$, $2a$ is the long side and $2b$ is the short side of the rectangle, and $\theta_d=\tan^{-1}(b/a)$. In the case of an ellipse, arbitrarily slow variation in geometry with rotation can be achieved in the limit $b/a\to 1$; this, however, is not possible for a rectangular mixer. The flows defined above are clearly time periodic with period $\pi/\omega$ which corresponds to half a revolution of the mixer.

Rescaling all lengths with $a$, time with $\omega^{-1}$, and velocities with $\omega a$, the equations for flow in dimensionless form are

$$\overline{v}_x=\frac{\overline{L}}{k}\left(1+\frac{\overline{y}}{\overline{\delta}}\right), \tag{10}$$

$$\overline{v}_y=-\overline{x}\left(\frac{\overline{y}}{\overline{\delta}}\right)^2, \tag{11}$$

with $\overline{\delta}=\overline{\delta}_0[1-(\overline{x}/\overline{L})^2]$. The variation of the dimensionless layer length with time for an ellipse is given by

$$\overline{L}(t)=\frac{\overline{b}}{(\overline{b}^2\cos^2\theta+\sin^2\theta)^{1/2}} \tag{12}$$

with $\theta=(\overline{t}+\alpha)\mathrm{mod}\,2\pi$, and for a rectangle by

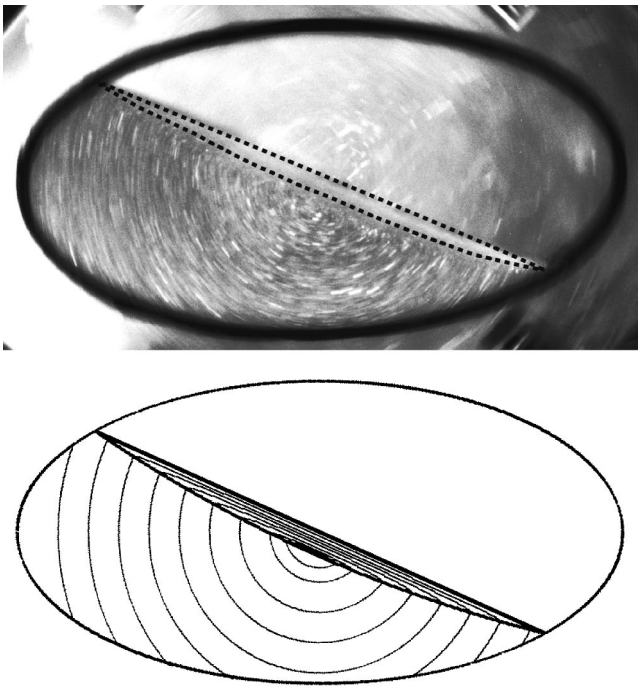

FIG. 3. Comparison of streaklines obtained experimentally for an ellipse with $\overline{b}=0.5$ (upper) with theoretically computed streamlines (lower). The dashed line demarcates the flowing layer in the upper photograph.

$$\overline{L}(t)=\begin{cases}\dfrac{1}{|\cos\theta|} & \text{if } \theta<\theta_d \text{ or } |\pi-\theta|<\theta_d \text{ or } \theta>(2\pi-\theta_d)\\ \dfrac{\overline{b}}{|\sin\theta|} & \text{otherwise}\end{cases} \tag{13}$$

with $\theta_d=\tan^{-1}\overline{b}$. The dimensionless parameters of the flow are then the aspect ratio ($\overline{b}=b/a$), and the maximum midlayer thickness ($\overline{\delta}_{0,\max}=k$, since $\overline{L}_{\max}=1$). The value of the parameter $k$ may be directly obtained from experimental results.

### C. Experiments

Flow visualization experiments are carried out in quasi-2D mixers of different shapes and sizes using spherical glass beads of diameter 0.8 mm (Quackenbush). Each mixer's front plate is glass and the rear plate is aluminum and grounded to prevent buildup of static electric charge. The thickness of all the mixers is 6 mm (~8 particle diameters). The mixers are rotated at a fixed angular speed in the rolling regime using a computer controlled stepper motor (Compumotor). Digital photographs are taken of the rotating mixers, which are half filled with the glass beads, using a computer controlled charge-coupled device camera (Kodak Megaplus). Relatively low shutter speeds are used to generate streaklines resulting from the particle motion. The digital images are analyzed for the layer thickness profiles and the midlayer thickness.

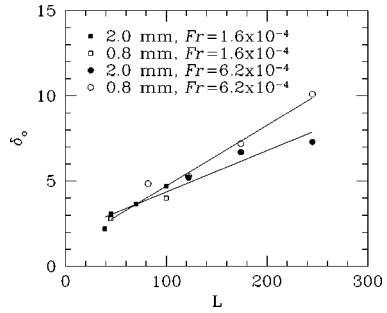


FIG. 4. Variation of the dimensionless midlayer thickness, $\delta_0/d$, with the dimensionless length of the free surface, $L/d$, for different bead sizes, $d$, and accelerations given in terms of the Froude number, $\mathrm{Fr}=\omega^2 L/g$.

### D. Results and discussion

Figure 3 shows a typical streakline photograph for an ellipse with a ratio of the minor to major axis given by $\bar{b}=0.5$. The layer, comprising the faster moving particles is clearly visible. Particles in the bed move along circular arcs, and the interface between the bed and the layer (the dashed line in Fig. 3) is obtained by joining the points at which an abrupt change in the direction of motion occurs. Streamlines predicted by the model for the corresponding layer thickness are shown alongside (Fig. 3). The streamlines are computed by numerically integrating the following equations:

$$\frac{d\bar{x}}{ds}=\bar{v}_x(\bar{x},\bar{y},\bar{t}), \tag{14}$$

$$\frac{d\bar{y}}{ds}=\bar{v}_y(\bar{x},\bar{y},\bar{t}), \tag{15}$$

keeping $\bar{t}$ fixed, where $(\bar{v}_x,\bar{v}_y)$ is the velocity in the bed and the layer, and $s$ is a dummy variable. There is good agreement between theory and experiment. Photographs taken at different mixer orientations show that the angle of the free surface is independent of the rotation of the mixer. This validates our assumption that the surface position is constant with time.

Figure 4 shows the variation of the midlayer thickness ($\delta_0$) with length of the layer ($L$) obtained experimentally using different mixers, and for two different accelerations expressed in dimensionless form in terms of the Froude number. The data for each value of the acceleration fall on a straight line, which validates the assumption of geometrical similarity of the layer ($k=\delta_0/L\equiv$constant).

Computed streamlines for an ellipse and a square at different orientations are shown in Fig. 5. The regions in which transverse intersection between streamlines occurs are shaded. The condition of intersection of streamlines, required for chaotic advection in 2D time-periodic flows is clearly satisfied in both cases.

## III. TRANSVERSE MIXING

We consider the transverse mixing in noncircular containers by means of computations based on the flow model discussed in Sec. II. The dimensionless governing equations for the calculation of a trajectory in the layer are

$$\frac{d\bar{x}}{d\bar{t}}=\bar{v}_x(\bar{x},\bar{y},\bar{t}), \tag{16}$$

$$\frac{d\bar{y}}{d\bar{t}}=\bar{v}_y(\bar{x},\bar{y},\bar{t})+w(t), \tag{17}$$

where $(\bar{v}_x,\bar{v}_y)$ is the velocity field given in Eqs. (10) and (11), and $w(t)$ is a white noise term that simulates particle diffusion. The above equations are the Lagrangian representation of the convective diffusion equation, neglecting diffusion relative to the convection in the flow direction ($\bar{x}$). The time integral of the white noise term at different times,

$$S(\Delta\bar{t})=\int_{\bar{t}}^{\bar{t}+\Delta\bar{t}} w(t')dt', \tag{18}$$

gives a set of Gaussian random numbers, $\{S\}$, which are related to the dimensionless particle collisional diffusivity by $\langle S^2\rangle=2\bar{D}_{\mathrm{coll}}\Delta\bar{t}$, where the pointed brackets denote an average over the set. The collisional diffusivity is made dimensionless with $\omega a^2$. The motion of the particles in the bed is simply obtained as a map corresponding to the rotation about point $P$. The above formulation allows for detailed analysis of the mixing in containers of different geometry. We note that segregation can be incorporated in the above framework,

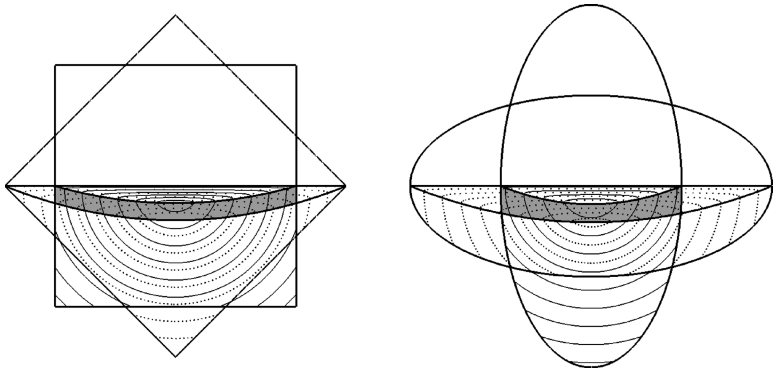

FIG. 5. Computed streamlines for a square and an elliptical mixer at different orientations. The shaded region in each case shows the region in which transverse intersections between the streamlines at the different orientations occur.

as shown in Ref. 24 for a mixture of different density particles in a rotating cylinder. The inclusion of these effects is, however, beyond the scope of this paper.

### A. Computational details

Computations allow the study of advection in isolation (no diffusion), whereas it is difficult, as we shall see, to devise laboratory experiments in which particle diffusion effects are negligibly small. We study advection in the mixers in two ways: (i) by computation of *Poincaré sections*, stroboscopic maps of (continuum) particle trajectories, and (ii) blob deformation. The Poincaré sections are obtained from computing the particle trajectories by integration of the velocity field with respect to time [Eqs. (16) and (17) with $w(\bar{t})=0$], and noting the position after each half revolution of the mixer. Several different initial conditions are used in generating the Poincaré sections so as to map out the flow behavior over the entire flow domain. Blob deformation computations are carried out by mapping a large number of particles, initially uniformly distributed in a circular region, by integration of the velocity field for the specified time duration, for each of the particles.

Computational results and experiments show that particle collisional diffusion has a significant effect on mixing. Computational studies of blob deformation involving advection and diffusion in the 2D noncircular mixers are carried out to understand their relative importance in the present case. The computational procedure used is similar to that used for blob deformation in the limit of pure advection. In addition, particles flowing in the layer are given random Gaussian displacements with variance $2\bar{D}_{\mathrm{coll}}\Delta\bar{t}$ to simulate diffusion; $\Delta\bar{t}$ is the integration time step. The particle collisional diffusivity is estimated from the following scaling relation obtained by Savage[34] from particle dynamics computations for shear flow

$$D_{\mathrm{coll}}=f(v)d^2\frac{dv_x}{dy}, \tag{19}$$

where $d$ is the particle diameter and $v$ is the solids volume fraction. For $v=0.55$ and a coefficient of restitution about 0.9, which correspond roughly to the parameters for the system under consideration, the prefactor in Eq. (19) is $f(v)\approx 0.025$.[34] On substitution of the dimensionless velocity using Eq. (10), after casting Eq. (19) in dimensionless form, we get

$$\bar{D}_{\mathrm{coll}}=0.025\frac{\bar{d}^2}{\bar{k}^2}, \tag{20}$$

where $\bar{d}=d/a$. In obtaining Eq. (20), we use the relationship $\bar{\delta}_0=k\bar{L}$, and evaluate the velocity gradient at the midpoint of the layer ($\bar{x}=0$). In general, the collisional diffusivity varies with granular temperature (mean kinetic energy associated with the velocity fluctuations) and solids volume fraction in the layer. Here, for simplicity, we take the diffusivity to be a constant as given by Eq. (20). Previous studies have shown that Eq. (20) gives reasonable predictions of mixing in the system.[10,24]

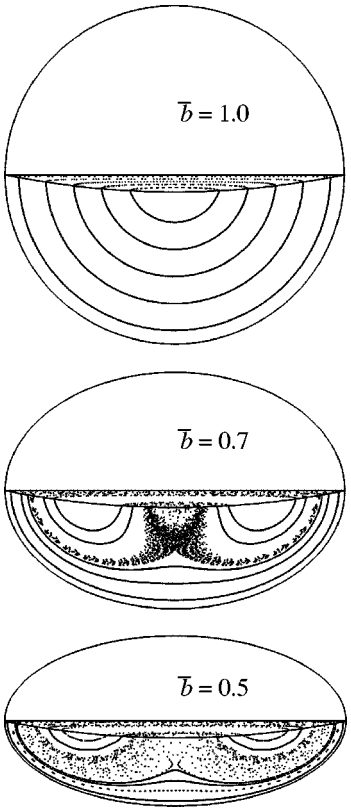


FIG. 6. Poincaré sections for elliptical mixers of varying aspect ratio ($\bar{b}$). The dimensionless midlayer thickness used in the computations is $\bar{\delta}_{0,\max}=0.1$.

### B. Experiments

Experimental studies of blob deformation are also carried out to get an insight into the mixing process. A circular blob of colored beads is carefully positioned at the desired location in the bed. The mixer is rotated at a constant angular speed by means of the stepper motor, and digital photographs are taken at different times to record the progress of mixing.

Quantitative comparisons between theory and experiment are made in terms of the intensity of segregation, which is essentially the normalized standard deviation of the concentration of tracer particles from the value for perfect mixing.[35] The intensity of segregation is obtained from the experimental photographs by thresholding the digital photograph and determining the fraction of the area occupied by the colored particles in each of a grid of squares placed over the mixer. The fraction is taken to be the local concentration, and the intensity of segregation is calculated as the standard deviation of the concentration from the mean value.[36]

### C. Results and discussion

Consider the case of pure advection first. Figure 6 shows Poincaré sections for ellipses of different aspect ratios. For a circular mixer ($\bar{b}=1$) the Poincaré section shows only regular motion, and the invariant curves obtained (KAM curves[26]) coincide with the streamlines. However, for lower values of the aspect ratio ($\bar{b}<1$), regions of chaotic motion

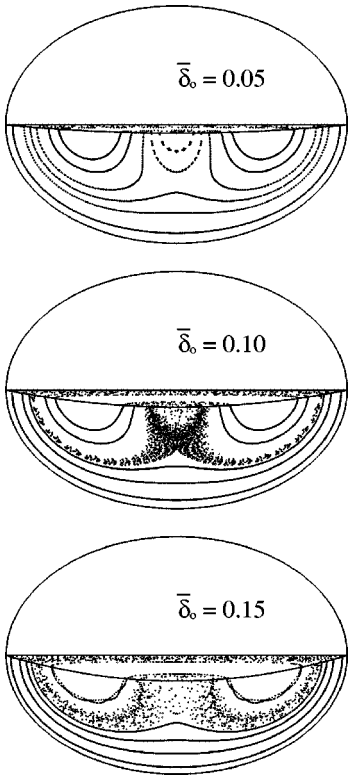


FIG. 7. Poincaré sections for elliptical mixers of varying layer thickness. The aspect ratio of the ellipse used in the computations is $\bar{b} = 0.7$.

are interspersed with regions of regular motion (demarcated by KAM curves); the size of the chaotic regions increases with decreasing aspect ratio ($\bar{b}$). Figure 7 shows the effect of layer thickness for a fixed value of the aspect ratio. Thicker layers produce more widespread chaos; this is because the area in which transverse intersections between streamlines at different mixer orientations occur (the shaded area in Fig. 5) increases with layer thickness.

A comparison of blob deformation in three different geometries (square, ellipse, and circle) is shown in Fig. 8. The initial positions of the blobs and the Poincaré sections for the mixers are included as insets in Fig. 8. In the circular mixer, each blob is deformed into a filament; the length of the filaments increases slowly with time. In contrast, markedly different behavior is seen for elliptical and square mixers. The initially circular blobs in the chaotic regions are deformed into filaments, which fold back upon themselves repeatedly. This indicates the presence of an underlying homoclinic structure which is characteristic of chaotic advection. The blobs in the regular regions of these mixers remain largely undeformed (the other signatures of chaos are a positive Liapunov exponent—exponential stretching—and the presence of horseshoe maps; the rate of stretching is considered in Fig. 9).

The major qualitative difference between mixing by regular and chaotic advection is illustrated in Fig. 9. The change in the computed perimeter length of the blob increases linearly with time in the circular mixer, whereas an exponential increase of length with time is obtained for the blobs in the chaotic regions of the square and elliptical mixers. The latter is a signature of a chaotic flow.

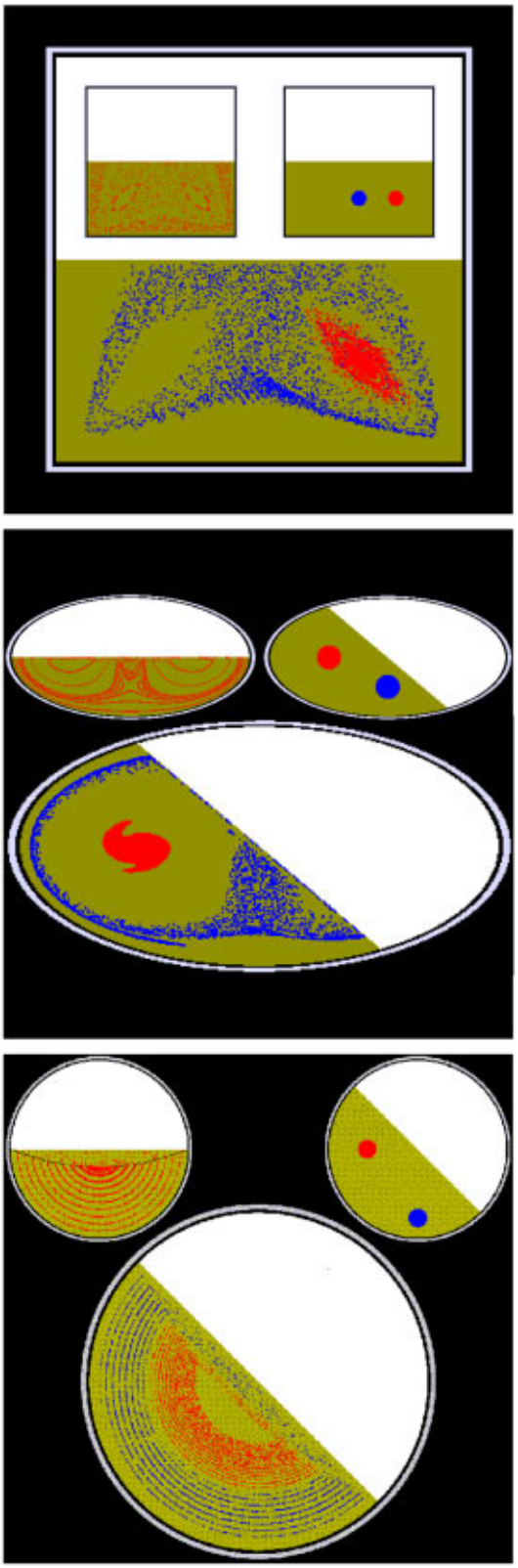

FIG. 8. Comparison of the mixing of tracer particles in a circular, elliptical, and square mixer simulated using the model with no particle diffusion. The inset figure on the upper left-hand side shows the Poincaré section, and the initial condition is shown in the upper right-hand inset.

Comparison between the mixing in the square and elliptical mixers shows that the square has more widespread chaos and the rate of stretching is also higher.

Diffusion acts to blur the structures formed by advection

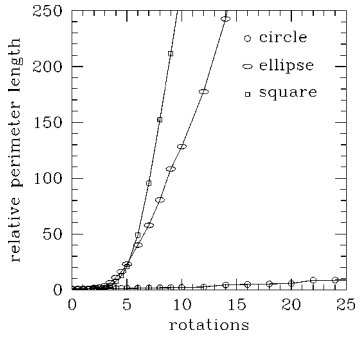


FIG. 9. Variation of the relative perimeter length of a blob with time in the mixers corresponding to the computation in Fig. 8. Note that while the perimeter length in the circular mixer grows linearly, the length in the non-circular mixers grows exponentially.

of a blob, and thus enhances mixing. Figure 10 shows the effect of increasing diffusivity on the deformation of a blob in an elliptical mixer. While the shape of the blob is considerably altered by diffusion, the stretching of the blob, as may be expected, is along the unstable manifold (refer to the Poincaré section in Fig. 10) as in the case with no diffusion. The experimentally mixed state is also shown in Fig. 10. There is good agreement between theory and experiment for the case corresponding to the diffusivity calculated from Eq. (20). Note also that chaos does not imply that stretching takes place immediately; after three revolutions the stretching of the circular blob is relatively small.

A more detailed comparison between theory and experiment is shown in Fig. 11 for blob deformation in a square mixer. There is good qualitative agreement between the two in terms of the structures produced by mixing. Comparison to the Poincaré section obtained excluding collisional diffusion (Fig. 8, inset) shows that several features of the structure are apparent even when diffusion is included: blobs are stretched along manifolds, and the density of particles in the regular islands is small. A quantitative comparison between theory and experiment is shown in Fig. 12. There is again good agreement between the two for the variation of intensity of segregation with time. We note that there is no adjustable parameter in the model.

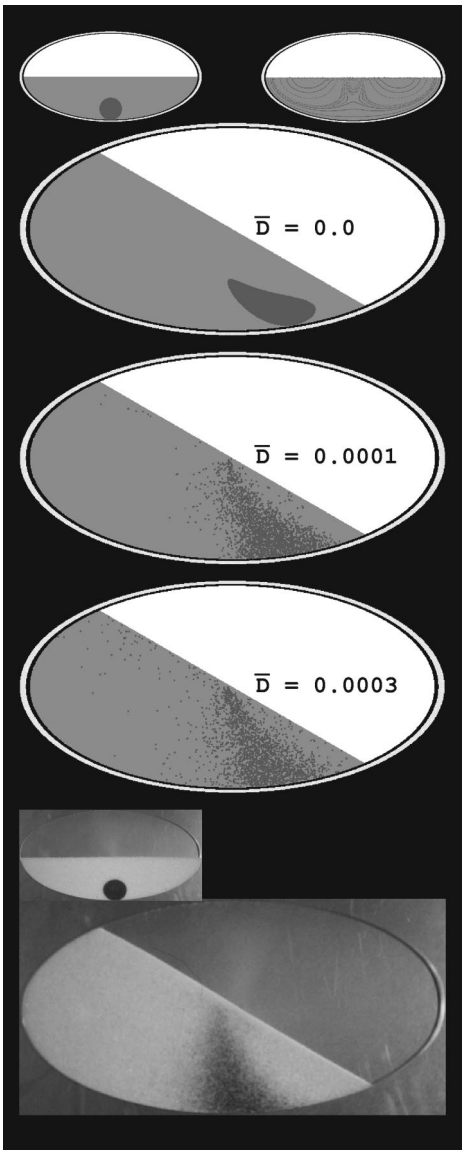


FIG. 10. Effect of diffusion on blob deformation is shown by means of computations for various values of the dimensionless diffusivity ($\bar{D}$) for three mixer revolutions. The initial condition is shown as an inset on the left-hand side and the Poincaré section as an inset on the right-hand side. Deformation of a blob after three revolutions obtained experimentally is shown at the bottom with the initial distribution of the particles inset.

## IV. SCALE UP OF TUMBLING MIXERS

Experimental results for the elliptical and square mixers discussed above indicate that diffusion is sufficiently fast so as to obliterate the folded structures seen in Fig. 8. This could be taken to seem to indicate that chaotic advection is of little utility in the presence of relatively fast particle diffusion. However, diffusional effects are scale dependent, and their relative importance with respect to advection can be estimated in terms of the Péclet number for the system under consideration. For the tumbling mixers discussed above, the Péclet number is defined as the ratio of the characteristic diffusion time, $\delta_0^2/D_{\text{coll}}$, to the characteristic advection time, $L/u$, and is given by

$$\text{Pe}=\frac{\delta_0^2 u}{LD_{\text{coll}}}. \tag{21}$$

Using $\delta_0=kL$, and Eq. (19) for the collisional diffusivity, we obtain

$$\text{Pe}=20k^3\left(\frac{L}{d}\right)^2. \tag{22}$$

Thus the Péclet number increases, and therefore the effectiveness of the diffusion decreases with increasing system size. The Péclet number for the experimental systems discussed in Sec. III is $\text{Pe}\approx 100$.

We illustrate the above results by means of computations comparing the mixing in square and circular mixers, for large and small sized containers. Figure 13 shows the variation of the intensity of segregation with time for four different mixers and two different initial conditions. In one case, 13(b), the initial distribution corresponds to the left-half of

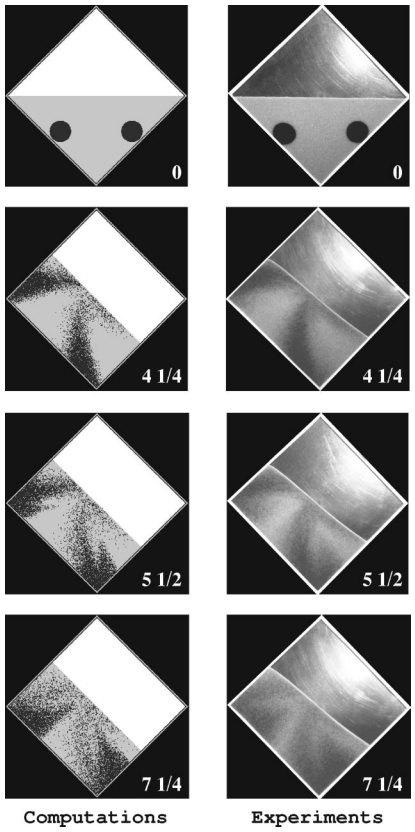


FIG. 11. Mixing of tracer particles in a container with a square cross section. Shown is a comparison of an experiment using colored glass beads (the right-hand side) and a simulation using the model. The number of rotations for each image is listed in the corner.

the bed containing colored particles and the right-half of the bed white particles; the other (somewhat more practical) to one material layered on top of the other [13(a)]. The intensity of segregation for all cases is initially equal to 0.5, which corresponds to the theoretical value for a completely segregated mixture containing 50% of the colored particles. The decay in intensity of segregation with time for the different mixers is, however, very different. One of the initial conditions favors the circular geometry. A good mixer however, should mix well regardless of the initial condition and the horizontally layered case makes it clear that the circle is a poor mixer. Moreover, in the case of the circular mixer, in

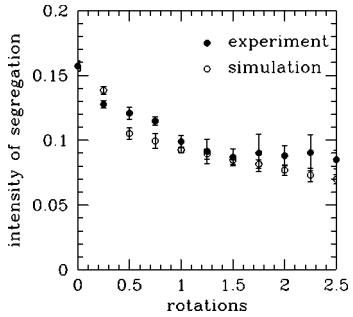


FIG. 12. Variation of the intensity of segregation vs mixer rotation is shown for the experimental and theoretical results in Fig. 11. The filled circles represent experimental values and the open circles denote values obtained from the model.

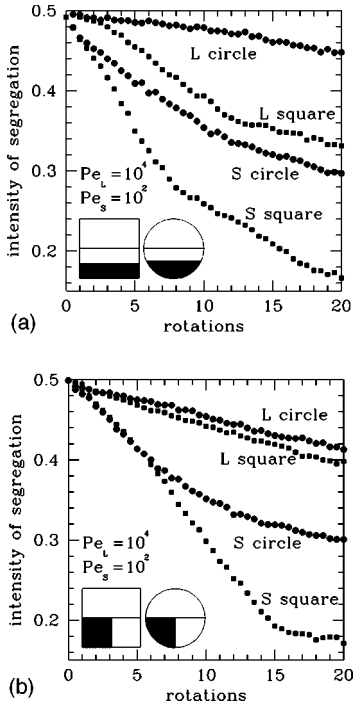


FIG. 13. Variation of the intensity of segregation vs mixer rotation obtained for mixers of different shapes and sizes by computations. The large systems correspond to a Péclet number $Pe_L = 10^4$, and the small systems to $Pe_S = 10^2$, which indicates a mixer size ratio of 10. Two initial conditions, shown as insets, are considered.

which mixing is primarily by diffusion across streamlines, increase in the mixer size results in a significant reduction in the rate of mixing. In contrast, for the square mixer, in which chaotic advection aids diffusion, there is a smaller reduction in mixing rate with mixer size. Furthermore, comparing at equal sizes (i.e., equal Péclet numbers) we see that the square container mixes faster than the circular one for both the sizes considered here. Thus, in addition to the Péclet number, mixer shape significantly affects the rate of mixing.

The results presented above indicate that chaotic advection becomes more important with increasing mixer size. Selection of an appropriate (noncircular) geometry may thus be useful for fast transverse mixing in large mixers, given the decreasing importance of diffusion with size.

## V. CONCLUSIONS

The flow model for noncircular two-dimensional mixers presented here forms the basis of the analysis of mixing of granular materials by chaotic advection and diffusion. As developed, the model is appropriate for the flows in mixers with arbitrary shape, but which are symmetric with respect to half rotations. Computational studies of mixing by advection alone (no diffusion) show chaotic mixing for noncircular mixers as evidenced by Poincaré sections and exponential length stretch. Thicker flowing layers and greater deviation of the mixer cross-sectional shape from circular increase the area of the regions of chaos.

Diffusion plays an important role in the mixing of granular materials; experiments and computations for the laboratory scale mixers studied here show that diffusion blurs the

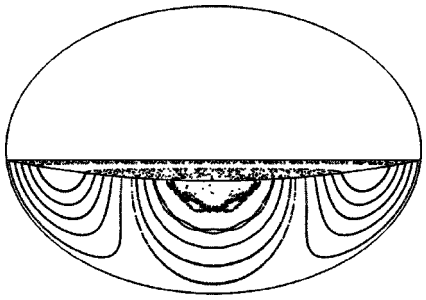

FIG. 14. Poincaré section for an elliptical mixer, which is less than half full (the top surface is at a distance $h=0.05a$ from the centroid). The aspect ratio and the layer thickness used in the computation are $\bar{b}=0.7$ and $\bar{\delta}_{0,\max}=0.1$. Figure 6 for the Poincaré section corresponding to the half full case. The model used for the computations is essentially the same as that for a half-full mixer, but taking into account the up and down motion of the interface. Momentum effects are neglected in the model.

structures produced by chaotic advection. However, structures corresponding to the Poincaré sections are evident in these cases. Chaotic advection aids diffusion and results in faster overall mixing as compared to the mixing in a circular mixer of the same size. Furthermore, scaling shows that diffusion becomes less important relative to chaotic advection with increasing mixer size. Chaotic mixing is thus essential for practical applications, given that large mixers are the norm in industrial processes. The scaling study also indicates the importance of correctly identifying contributions of advection and diffusion in the scaling up of tumbling mixers. While there is little reduction in the rate of mixing with increase in size for square mixers, this is not true for circular mixers in which diffusion is dominant.

Although the results presented in this paper pertain to a specific example, the conclusions are valid for the more general case as well. For example, Fig. 14 shows the Poincaré section for an elliptical mixer, which is slightly less than half full using essentially the same model as presented in the paper. In this case the bed height varies periodically with time. The velocity generated by this variation is included in the model. Regions of chaos are evident in this case as well. Using nonsymmetric mixers would introduce a greater deviation from the geometry of poor mixing typical of circular containers than the mixers considered here, and would perhaps produce more widespread chaotic advection.

In hindsight, existing processes undoubtedly already contain elements of chaotic advection (e.g., in V-blenders or double-cone blenders);[36] however, without explicit recognition of the underlying reasons for mixing successes and failures (global chaos versus large-scale regular islands), optimization of such devices is impossible. While previous results from fluid mixing would be useful for analysis of granular mixing, more studies focusing on the special aspects of granular flows (e.g., flow in thin layers) and their implications for chaotic advection are needed.

Another crucial aspect should be mentioned as well. Perhaps the most important difference between the mixing of fluids and the mixing of solids is segregation: In granular materials mixing and segregation occur in parallel. In solids, more ''agitation''—tumbling in our case—does not imply better mixing. Granular mixtures of dissimilar materials often segregate when tumbled.[24] In the case of the circular mixer time-independent isoconcentration regions of segregated materials coincide with the streamlines. The chaotic scenario outlined here suggests a wealth of unexplored possibilities: a dynamic balance between chaotic advection trying to destroy large scale inhomogeneities and the de-mixing caused by segregation.

## ACKNOWLEDGMENTS

This work was supported by the Department of Energy, Division of Basic Energy Sciences, and the National Science Foundation, Fluid, Particle and Hydraulic Systems.

[1] B. J. Ennis, J. Green, and R. Davies, ''The legacy of neglect in the United States,'' Chem. Eng. Prog. **90**, 32–43 (1994); J. Bridgwater, ''Particle technology,'' Chem. Eng. Sci. **50**, 4081–4089 (1995).
[2] G. Shanmugan *et al.*, in ''Sequence Stratigraphy in British Geology,'' edited by S. P. Heselbo and D. N. Parkinson, Geological Society Special Publ. No. 103, pp. 145–175 (1996).
[3] P. M. C. Lacey, ''Developments in the theory of particle mixing,'' J. Appl. Chem. **4**, 257–268 (1954).
[4] J. Bridgwater, ''Fundamental powder mixing mechanisms,'' Powder Technol. **15**, 215–231 (1976); L. T. Fan, Y. Chen, and F. S. Lai, ''Recent developments in solids mixing,'' *ibid.* **61**, 255–277 (1990).
[5] L. T. Fan, S. J. Chen, and C. A. Watson, ''Solids mixing,'' Ind. Eng. Chem. **62**, 53–69 (1970).
[6] F. J. Muzzio, P. Robinson, C. Wightman, and D. Brone, ''Sampling practices in powder blending,'' Int. J. Pharm. **155**, 153–178 (1997).
[7] J. M. Ottino, ''Mixing, chaotic advection, and turbulence,'' Annu. Rev. Fluid Mech. **22**, 207–54 (1990).
[8] G. Metcalfe, T. Shinbrot, J. J. McCarthy, and J. M. Ottino, ''Avalanche mixing of granular materials,'' Nature (London) **374**, 39–41 (1995).
[9] R. Hogg and D. W. Fuerstenau, ''Transverse mixing in a rotating cylinder,'' Powder Technol. **6**, 139–145 (1972); I. Inoue, K. Yamaguchi, and K. Sato, ''Motion of a particle and mixing process in a horizontal drum mixer,'' Kagaku (Kyoto) **34**, 1323–1330 (1970).
[10] D. V. Khakhar, J. J. McCarthy, T. Shinbrot, and J. M. Ottino, ''Transverse flow and mixing of granular materials in a rotating cylinder,'' Phys. Fluids **9**, 31–43 (1997).
[11] R. Hogg, D. S. Cahn, T. W. Healy, and D. W. Fuerstenau, ''Diffusional mixing in an ideal system,'' Nature (London) **209**, 494–496 (1966); ''Diffusional mixing in an ideal system,'' Chem. Eng. Sci. **21**, 1025–1035 (1966).
[12] S. J. Rao, S. K. Bhatia, and D. V. Khakhar, ''Axial transport of granular materials in a rotating cylinder. 2 Experiments in a non-flow system,'' Powder Technol. **67**, 153–160 (1992).
[13] G. A. Kohring, ''Studies of diffusional mixing in rotating drums via computer simulations,'' J. Phys. I **5**, 1551–1561 (1995).
[14] H. Henein, J. K. Brimacombe, and A. P. Watkinson, ''Experimental study of transverse bed motion in rotary kilns,'' Metall. Trans. B **14**, 191–197 (1983).
[15] J. C. Williams, ''The segregation of particulate materials,'' Powder Technol. **15**, 245–256 (1976).
[16] M. B. Donald and B. Roseman, ''Mixing and de-mixing of solid particles. I,'' Br. Chem. Eng. **7**, 749–752 (1962).
[17] N. Nityanand, B. Manley, and H. Henein, ''An analysis of radial segregation for different sized spherical solids in rotary kilns,'' Metall. Trans. B **17**, 247–255 (1986).
[18] S. Das Gupta, D. V. Khakhar, and S. K. Bhatia, ''Axial segregation of particles in a horizontal rotating cylinder,'' Chem. Eng. Sci. **46**, 1513–1520 (1991).
[19] O. Zik, D. Levine, S. G. Lipson, S. Shtrikman, and J. Stavans, ''Rotationally induced segregation of granular materials,'' Phys. Rev. Lett. **73**, 644–647 (1994).
[20] K. M. Hill and J. Kakalios, ''Reversible axial segregation of rotating granular media,'' Phys. Rev. E **52**, 4393–4400 (1995).
[21] C. M. Dury and G. H. Ristow, ''Radial segregation in a two-dimensional rotating drum,'' J. Phys. I **7**, 737–745 (1997).
[22] M. H. Cooke and J. Bridgwater, ''Interparticle percolation: A statistical

mechanical interpretation,'' Ind. Eng. Chem. **18**, 25–31 (1979).
[23] S. B. Savage and C. K. K. Lun, ''Particle size segregation in inclined chute flow of dry cohesionless granular materials,'' J. Fluid Mech. **189**, 311–335 (1988).
[24] D. V. Khakhar, J. J. McCarthy, and J. M. Ottino, ''Radial segregation of granular materials in rotating cylinders,'' Phys. Fluids **9**, 3600–3614 (1997).
[25] S. S. Hsiau and M. L. Hunt, ''Granular thermal diffusion in flows of binary sized mixtures,'' Acta Mech. **114**, 121–137 (1996).
[26] J. M. Ottino, *The Kinematics of Mixing: Stretching, Chaos, and Transport* (Cambridge University Press, Cambridge, 1989); J. M. Ottino, F. J. Muzzio, M. Tjahjadi, J. G. Franjione, S. C. Jana, and H. A. Kusch, ''Chaos, symmetry and self-similarity: Exploiting order and disorder in mixing processes,'' Science **257**, 754–760 (1992).
[27] J. Rajchenbach, ''Flow in powders: From avalanches to continuous regime,'' Phys. Rev. Lett. **65**, 2221–2223 (1990).
[28] M. Nakagawa, S. A. Altobelli, A. Caprihan, E. Fukushima, and E. K. Jeong, ''Noninvasive measurements of granular flows by magnetic resonance imaging,'' Exp. Fluids **16**, 54–60 (1993).
[29] J. Rajchenbach, E. Clement, and J. Duran, in *Fractal Aspects of Materials*, edited by F. Family, P. Meakin, B. Sapoval, and R. Wool, 1995.
[30] G. Baumann, I. M. Janosi, and D. E. Wolf, ''Surface properties and flow of granular material in a 2d rotating drum model,'' Phys. Rev. E **51**, 1879–1888 (1995).
[31] V. Buchholtz, T. Poschel, and H. J. Tillemans, ''Simulation of rotating drum experiments using non-circular particles,'' Physica A **216**, 199–204 (1995).
[32] G. H. Ristow, ''Dynamics of granular materials in rotating drums,'' Europhys. Lett. **34**, 263–268 (1996).
[33] T. Elperin and A. Vikhansky, ''Kinematics of the mixing of granular material in slowly rotating containers,'' Europhys. Lett. **43**, 17–22 (1998).
[34] S. B. Savage, Disorder, in *Disorder and Granular Media*, edited by D. Bideau and A. Hansen (Elsevier Science, Amsterdam, 1993), pp. 255–285.
[35] P. V. Danckwerts, ''The definition and measurement of some characteristics of mixtures,'' Appl. Sci. Res., Sect. A **3**, 279–296 (1952).
[36] M. Poux, P. Fayolle, J. Bertrand, D. Bridoux, and J. Bousquet, ''Powder mixing—some practical rules applied to agitated systems,'' Powder Technol. **68**, 213–234 (1991).